



Virginia Commonwealth University
VCU Scholars Compass

Chemistry Publications

Dept. of Chemistry

2011

Structure and hydration of the $C_4H_4 \bullet+$ ion formed by electron impact ionization of acetylene clusters

Paul O. Momoh

Virginia Commonwealth University

Ahmed Hamid

Virginia Commonwealth University

Samuel A. Abrash

Virginia Commonwealth University

M. Samy El-Shall

Virginia Commonwealth University, mseishal@vcu.edu

Follow this and additional works at: http://scholarscompass.vcu.edu/chem_pubs

 Part of the [Chemistry Commons](#)

Momoh, P. O., Hamid, A. M., & Abrash, S. A., et al. Structure and hydration of the C_4H_4 center $\bullet+$ ion formed by electron impact ionization of acetylene clusters. *The Journal of Chemical Physics*, 134, 204315 (2011). Copyright © 2011 American Institute of Physics.

Downloaded from

http://scholarscompass.vcu.edu/chem_pubs/54

This Article is brought to you for free and open access by the Dept. of Chemistry at VCU Scholars Compass. It has been accepted for inclusion in Chemistry Publications by an authorized administrator of VCU Scholars Compass. For more information, please contact libcompass@vcu.edu.

Structure and hydration of the $C_4H_4^{\bullet+}$ ion formed by electron impact ionization of acetylene clusters

Paul O. Momoh, Ahmed M. Hamid, Samuel A. Abrash,^{a)} and M. Samy El-Shall^{b)}
Department of Chemistry, Virginia Commonwealth University, Richmond, Virginia 23284-2006, USA

(Received 14 March 2011; accepted 30 April 2011; published online 27 May 2011)

Here we report ion mobility experiments and theoretical studies aimed at elucidating the identity of the acetylene dimer cation and its hydrated structures. The mobility measurement indicates the presence of more than one isomer for the $C_4H_4^{\bullet+}$ ion in the cluster beam. The measured average collision cross section of the $C_4H_4^{\bullet+}$ isomers in helium ($38.9 \pm 1 \text{ \AA}^2$) is consistent with the calculated cross sections of the four most stable covalent structures calculated for the $C_4H_4^{\bullet+}$ ion [methylene cyclopropene (39.9 \AA^2), 1,2,3-butatriene (41.1 \AA^2), cyclobutadiene (38.6 \AA^2), and vinyl acetylene (41.1 \AA^2)]. However, none of the single isomers is able to reproduce the experimental arrival time distribution of the $C_4H_4^{\bullet+}$ ion. Combinations of cyclobutadiene and vinyl acetylene isomers show excellent agreement with the experimental mobility profile and the measured collision cross section. The fragment ions obtained by the dissociation of the $C_4H_4^{\bullet+}$ ion are consistent with the cyclobutadiene structure in agreement with the vibrational predissociation spectrum of the acetylene dimer cation $(C_2H_2)_2^{\bullet+}$ [R. A. Relf, J. C. Bopp, J. R. Roscioli, and M. A. Johnson, *J. Chem. Phys.* **131**, 114305 (2009)]. The stepwise hydration experiments show that dissociative proton transfer reactions occur within the $C_4H_4^{\bullet+}(H_2O)_n$ clusters with $n \geq 3$ resulting in the formation of protonated water clusters. The measured binding energy of the $C_4H_4^{\bullet+}H_2O$ cluster, $38.7 \pm 4 \text{ kJ/mol}$, is in excellent agreement with the G3(MP2) calculated binding energy of cyclobutadiene $^{\bullet+} \cdot H_2O$ cluster (41 kJ/mol). The binding energies of the $C_4H_4^{\bullet+}(H_2O)_n$ clusters change little from $n = 1$ to 5 ($39\text{--}48 \text{ kJ/mol}$) suggesting the presence of multiple binding sites with comparable energies for the water- $C_4H_4^{\bullet+}$ and water-water interactions. A significant entropy loss is measured for the addition of the fifth water molecule suggesting a structure with restrained water molecules, probably a cyclic water pentamer within the $C_4H_4^{\bullet+}(H_2O)_5$ cluster. Consequently, a drop in the binding energy of the sixth water molecule is observed suggesting a structure in which the sixth water molecule interacts weakly with the $C_4H_4^{\bullet+}(H_2O)_5$ cluster presumably consisting of a cyclobutadiene $^{\bullet+}$ cation hydrogen bonded to a cyclic water pentamer. The combination of ion mobility, dissociation, and hydration experiments in conjunction with the theoretical calculations provides strong evidence that the $(C_2H_2)_2^{\bullet+}$ ions are predominantly present as the cyclobutadiene cation with some contribution from the vinyl acetylene cation. © 2011 American Institute of Physics. [doi:10.1063/1.3592661]

I. INTRODUCTION

Many complex organics including polycyclic aromatic hydrocarbons (PAHs) are present in flames and combustion processes as well as in outer space.¹⁻⁵ In fact, well over 100 organic molecules including acetylene, vinylacetylene, cyclobutadiene, benzene, and PAHs, are present in interstellar clouds, molecular clouds, solar nebulae, and in envelopes expelled by evolved stars.⁵⁻¹⁰ Gas phase polymerization, ion-molecule and intracuster reactions, and catalysis on nanoparticles are important synthetic pathways for the formation of complex molecules in the atmosphere and in space.^{5,11-14} In ion-molecule reactions, the processes of particular interest are those that lead to larger molecules, which may lead to the PAHs found in soot, meteorites and interstellar clouds.¹⁵⁻¹⁷

Intracuster ion-molecule reactions are uniquely suited for the discovery of novel catalytic pathways that can lead to the formation of complex organics. Since acetylene is the smallest organic molecule that can be polymerized, extensive studies have been focused on the ion chemistry of acetylene clusters not only due to the important roles of acetylene in flames and combustion processes including the mechanisms of soot formation, but also for the origin of larger molecular species such as benzene and polycyclic aromatic hydrocarbons (PAHs) in space.^{16,18-20} For example, the formation of benzene ions within ionized acetylene clusters, $(C_2H_2)^{\bullet+}_n$, has been suggested by several cluster studies conducted over many years.²¹⁻²⁸ Early experiments found the fragment ions observed from the photoionization of acetylene trimers to be identical to those obtained from other stable $C_6H_6^+$ isomers such as benzene, 2,4-hexadiyne, 1,3-hexadiyne, and 1,5-hexadiyne.²¹ However, photoelectron-photoion coincidence experiments and *ab initio* calculations showed that ionized acetylene dimer and trimer ions rearrange to produce

^{a)}Permanent Address: Department of Chemistry, University of Richmond, Richmond, VA 23173.

^{b)}Author to whom correspondence should be addressed. Electronic mail: mselshal@vcu.edu.

stable covalent core ions ($C_4H_4^{\bullet+}$ and $C_6H_6^{\bullet+}$, respectively) with a large release of energy that leads to loss of a neutral acetylene molecule from the ionized clusters.²³ Electron impact (EI) ionization of acetylene clusters $(C_2H_2)_n^+$ with n up to ~ 25 showed magic numbers at $n = 3$ and 14 which were attributed to the formation of benzene ($C_6H_6^{\bullet+}$) and $C_{28}H_{28}^{\bullet+}$ molecular ions, respectively.²⁴ Mass-selected ion mobility and collisional induced dissociation (CID) experiments coupled with theoretical calculations support the efficient formation of the benzene cations following the EI ionization of large acetylene clusters ($(C_2H_2)_n^{\bullet+}$ with n up to ~ 50).^{25,26} Ion hydration experiments show that the enthalpy and entropy changes for the stepwise hydration of the acetylene trimer cation are identical to those of the benzene cation.²⁶ Subsequent reactions of the benzene cation with acetylene molecules at higher temperatures (650 K) show evidence for sequential covalent addition leading to the formation of naphthalene-type ions.²⁷ Recently, Relph *et al.*, using infrared predissociation spectroscopy in conjunction with harmonic frequency calculations, showed that electron impact ionization of neutral $(C_2H_2)_n$ clusters results in the formation of a covalently bound $C_4H_4^{\bullet+}$ “core ion” which could lead to the presence of several isomers of the $n = 3$ species including a weak absorption attributed to the formation of the benzene cation.²⁸ This work suggests that the structure of the $C_4H_4^{\bullet+}$ ion could play an important role in the cluster-mediated ion chemistry.²⁸

In the present work, we report ion mobility experiments and theoretical studies aimed at elucidating the identity of the acetylene dimer ion, $(C_2H_2)_2^{\bullet+}$, formed by EI ionization of neutral acetylene clusters. The ion mobility approach requires a comparison of the average collision cross section calculated for likely structures to those formed in the experiment. We employed density functional theory (DFT) (Ref. 29) to determine lowest energy structures of the $C_4H_4^{\bullet+}$ potential energy surface. We also probe the thermochemical properties and reactivity of the $(C_2H_2)_2^{\bullet+}$ ion by measuring its hydration energies by one to six water molecules using equilibrium thermochemical measurements at different temperatures. The comparison of the stepwise hydration enthalpy and entropy changes of the acetylene dimer cation with the thermochemical data recently reported for the acetylene trimer cation²⁶ and the benzene cation³⁰ provides further evidence for the covalently bound structure of the $C_4H_4^+$ ion.

The organization of the paper is as follows. In Sec. II, we briefly describe the mass-selected ion mobility system and methods used for measuring the mobility and determining

the corresponding collision cross section of the mass-selected ions in helium. We also briefly describe the measurement of ion–molecule equilibrium and the determination of the stepwise enthalpy and entropy changes associated with the hydration of the $C_4H_4^{\bullet+}$ ion. The computational methods used for the structural calculations are briefly described in Sec. III. In Sec. IV, we present and discuss the results of the mass spectra, dissociation and mobility of the acetylene dimer ion $(C_2H_2)_2^{\bullet+}$. We also present the calculated structures of the $C_4H_4^{\bullet+}$ ion and utilize these structures to calculate collision cross sections of the $C_4H_4^{\bullet+}$ ion for comparison with the experimental cross sections obtained from the mobility measurements. This comparison provides the basis for suggesting the likely structures of the $C_4H_4^{\bullet+}$ ion involved in our experiments. Finally, we present the successive hydration enthalpy and entropy changes of the $C_4H_4^{\bullet+}$ ion with up to six water molecules and discuss the calculated hydrated structures with one and two water molecules. In Sec. V, we provide a brief summary of the results and highlight the new physical insights provided by this work on the structure and hydration of the $C_4H_4^{\bullet+}$ ion.

II. EXPERIMENTAL

The ion mobility, dissociation, and hydration experiments were performed using the VCU mass-selected ion mobility spectrometer. The details of the instrument can be found in several publications and only a brief description of the experimental procedure is given here.^{30–32}

Figure 1 illustrates the essential components of the ion mobility system. In the experiments, acetylene clusters were generated by supersonic expansion of a 2% acetylene/helium mixture (He ~ 4 atm). The mixture was passed through dry ice and moisture traps to diminish water vapor and acetone impurities (acetone is used as a stabilizing agent for pressurized acetylene). Typical ionizer electron energies ranged from 40 to 80 eV.

The ion mobility measurements are described in Sec. IV. For the ion hydration experiments, mass-selected $(C_4H_4^{\bullet+})$ ions were injected (in 5–15 μs pulses) into the drift cell containing 0.2–0.6 Torr of pure H_2O vapor. Flow controllers are used to maintain a constant pressure inside the drift cell. The temperature of the drift cell can be controlled to better than ± 1 K using four temperature controllers. Liquid nitrogen flowing through solenoid valves is used to cool down the drift cell. The reaction products can be identified by scanning a second quadrupole mass filter located coaxially after

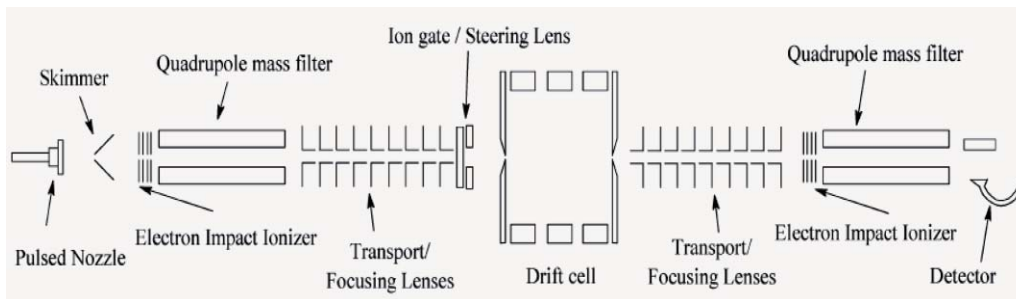


FIG. 1. Schematic diagram of the mass-selected ion mobility system at VCU.

the drift cell. The arrival time distributions (ATDs) are collected by monitoring the intensity of each ion as a function of time. The reaction time can be varied by varying the drift voltage. The injection energies (IEs) used in the experiments (5–20 eV, laboratory frame) are slightly above the minimum energies required to introduce the ions into the cell against the H₂O vapor outflow from the entrance orifice. Most of the ion thermalization occurs outside the cell entrance by collisions with the water vapor escaping from the cell entrance orifice. At a cell pressure of 0.2 Torr, the number of collisions that the C₄H₄^{•+} encounters with the water molecules within the 1.5 ms residence time inside the cell is about 10⁴ collisions, which is sufficient to ensure efficient thermalization of the C₄H₄^{•+} ions.

The ATDs of the injected C₄H₄^{•+} and the (C₄H₄^{•+})(H₂O)_n formed inside the cell are measured as a function of the drift voltage across the cell. The ion intensity ratio (C₄H₄^{•+})(H₂O)_n/(C₄H₄^{•+})(H₂O)_{n-1} is measured from the integrated peak areas of the ATDs as a function of decreasing cell drift field corresponding to increasing reaction times, and equilibrium is achieved when a constant ratio is obtained. Applying drift fields of 1–4 V/cm inside the drift cell at a temperature of 302 K and water pressure, P(H₂O), of 0.4 Torr corresponds to ion residence times between 0.4 and 3.0 ms, respectively. Under these conditions, equilibrium is ascertained by a constant (C₄H₄^{•+})(H₂O)_n/(C₄H₄^{•+})(H₂O)_{n-1} ratio and the equilibrium constants are then obtained using Eq. (1).

$$K_{\text{eq}} = \frac{I[\text{C}_4\text{H}_4^{\bullet+}(\text{H}_2\text{O})_n]}{I[\text{C}_4\text{H}_4^{\bullet+}(\text{H}_2\text{O})_{n-1}]P(\text{H}_2\text{O})}, \quad (1)$$

where *I* is the intensity of the ion peak taken from the integrated ATD. The equilibrium constants measured as a function of temperature yield Δ*H*[°] and Δ*S*[°] from the slopes and intercepts, respectively of the van't Hoff plots. All of the results are replicated three or more times.

III. THEORETICAL

Geometries and relative energies for a number of interesting isomers of the empirical formula C₄H₄⁺ were calculated using the unrestricted Perdew, Burke, and Enzerhof exchange and correlation functional (UPBEPBE) and the augmented correlation-consistent polarized valence double ζ basis set (aug-cc-pVDZ).³³ The aug-cc-pVDZ basis is a 5*s*2*p*/3*s*2*p* set for H, and a 10*s*5*p*2*d*/4*s*3*p*2*d* set for C. Likely geometry candidates for the dimer ions were derived from the known C₄H₄⁺ isomers obtained from the NIST databases.³⁴ All geometry optimizations were followed by vibrational frequency calculations to confirm all minima on the relevant potential energy surface. All relative energies were zero point energy (ZPE) corrected. All calculations were performed using the GAUSSIAN 03 suite of programs.³⁵

IV. RESULTS AND DISCUSSION

A. Mass spectra and dissociation of the acetylene dimer cation

Figure 2 displays a typical mass spectrum obtained by 46 eV EI ionization of neutral acetylene clusters formed by

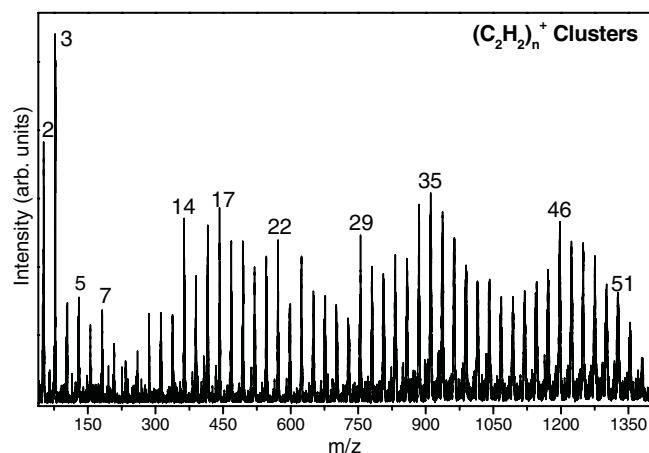


FIG. 2. Mass spectrum of EI ionized (46 eV) acetylene clusters.

supersonic expansion. The distribution of the cluster ions formed reveals some striking features corresponding to the enhanced intensities (magic numbers) for the (C₂H₂)_n^{•+} ions with *n* = 2, 3, 14, 17, 22, 29, 35, and 46. The strong magic numbers at *n* = 2 and 3 are consistent with previous work and suggest the formation of stable C₄H₄^{•+} and C₆H₆^{•+} ions in exothermic processes that can lead to extensive evaporation of neutral acetylene molecules from the cluster.^{21–24} The other magic numbers such as *n* = 14, 17, etc. probably reflect the solvation of the C₄H₄^{•+} and C₆H₆^{•+} ions with acetylene molecules where solvent shells are formed with specific numbers of the acetylene molecules. Others have hypothesized the isomerization of the (C₂H₂)₁₄^{•+} cluster to a covalent C₂₈H₂₈^{•+} ion.²⁴

Figure 3 displays the mass spectra obtained upon injection of the mass selected (C₂H₂)₂⁺ ions into the drift cell containing 0.46 Torr of He using different IEs. At lower IE (13 eV), no significant dissociation is observed except for the hydrogen loss to form the even-electron C₄H₃⁺ ion. The lack of dissociation is consistent with the formation of a covalent C₄H₄^{•+} ion as opposed to an ion–molecule acetylene dimer ion (C₂H₂)₂^{•+}. At high IE (53 eV), the observed fragments are C₄H₄^{•+}, C₄H₃⁺, C₄H₂^{•+}, C₄H⁺, C₃H₃⁺, C₂H₅⁺, C₂H₃⁺, C₂H₂^{•+}, and C₂H⁺ corresponding to *m/z* values of 52, 51, 50, 49, 39, 29, 27, 26, and 25 respectively. The observed fragments are in agreement with previous collision activated spectra of the C₄H₄^{•+} cation generated from different precursor molecules.³⁶ However, the observation of very minor fragments corresponding to the C₃H₃⁺ and C₃H₂^{•+} ions suggests that losses of CH and CH₂ units from the C₄H₄^{•+} cation are very unlikely. This suggests that the methylenecyclopropene and the 1,2,3-butatriene structures are not likely candidates for the C₄H₄^{•+} cation formed in our experiment. The apparent stability of the C₄H₄^{•+} ion towards dissociation (no dissociation observed with injection energies up to 20 eV) and the dominant high energy dissociation channels involving the loss of 1, 2, and 3 hydrogen atoms provide some support for the cyclobutadiene structure.

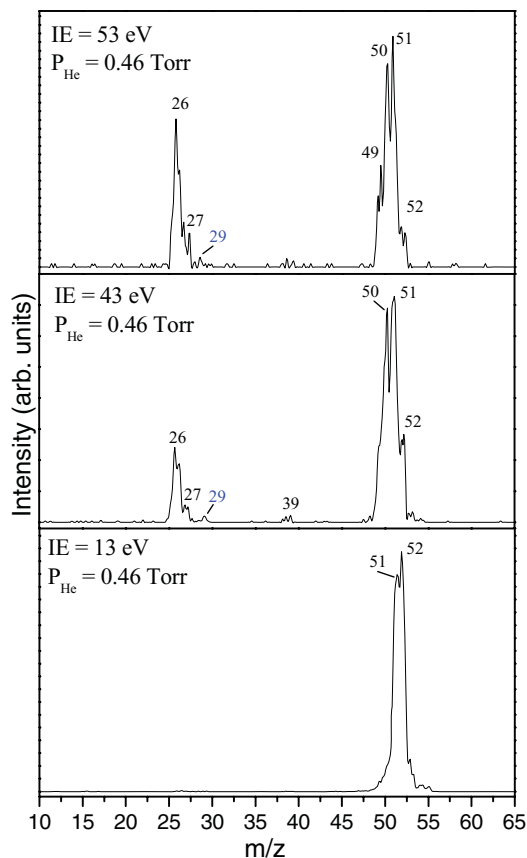


FIG. 3. Dissociation patterns resulting from the injection of mass selected $(\text{C}_2\text{H}_2)_2^{+\bullet}$ ions into the drift cell containing 0.46 Torr helium at 298 K using different injection energies (IEs, eV).

B. Mobility of the acetylene dimer cation

The mobility K of an ion is defined as:³⁷

$$K = \frac{v_d}{E}, \quad (2)$$

where E is the drift field ($E = V/z$, V is the drift voltage, and z is the length of the cell (cm)) and v_d is the drift velocity ($v_d = z/t_d$, t_d is the drift time in s). In order to effectively compare mobility measurements at different cell conditions or different instruments, K is normalized to standard conditions (STP) and referred to as reduced mobility, K_o .

$$K_o = K \left(\frac{273.15}{T} \right) \left(\frac{P}{760} \right). \quad (3)$$

Here, T is the buffer gas temperature (K) and P is the buffer gas pressure (Torr). Combination of Eqs. (2) and (3) gives

$$t_d = \left(\frac{z^2 \times 273.15}{T \times 760 \times K_o} \right) \left(\frac{P}{V} \right) + t_o, \quad (4)$$

where t_o is the effective time spent outside the drift cell. A plot of the drift time (t_d) versus P/V gives a straight line with slope containing K_o and an intercept corresponding to t_o . In the experiment, a packet of the mass selected ions of interest is injected into the drift cell and the arrival time distribution (ATD) is collected at varying cell voltages, V (with T and P held constant). All the mobility measurements were carried out in the low-field limit where the ion's drift velocity

is small compared to the thermal velocity and the ion mobility is independent of the field strength ($E/N < 6.0$, where E is the electric field intensity and N is the gas number density and E/N is expressed in units of Townsend (Td), where $1 \text{ Td} = 10^{-17} \text{ V cm}^2$).³⁷

The average collision cross section, $\Omega^{(1,1)}$, of the ions in the helium buffer gas is calculated according to the kinetic theory:

$$K = \frac{3qe}{16N} \left(\frac{2\pi}{k_B T_{\text{eff}}} \right)^{1/2} \left(\frac{M_i + M_b}{M_i M_b} \right)^{1/2} \frac{1}{\Omega_{\text{avg}}^{(1,1)}}, \quad (5)$$

where qe is the ion charge, N is the number density of the buffer gas, T_{eff} is the effective temperature, M_i and M_b are the masses of the ion and buffer gas, respectively, and $\Omega_{\text{avg}}^{(1,1)}$ is the orientationally averaged collision integral.

Figure 4 displays the ATDs for the mass selected $(\text{C}_2\text{H}_2)_2^{+\bullet}$ ions measured at various cell voltages. The inset in Fig. 4 shows a plot of t_d versus P/V with the solid line representing the least square fitting to the data points. The resulting reduced mobility K_o is determined to be $14.2 \pm 0.4 \text{ cm}^2 \text{ V}^{-1} \text{ s}^{-1}$ which corresponds to a collision cross section in helium of $\Omega = 38.9 \pm 1.4 \text{ \AA}^2$.

The ATDs of the injected ions are calculated for a finite packet of ions, $\phi(t)$, exiting a cylindrical drift tube through an aperture area (a) of $78.5 \mu\text{m}^2$ using the transport Eq. (6):³⁸

$$\phi(t) = \frac{sa e^{-\alpha t}}{4\sqrt{\pi} D_L t} \left(v_d + \frac{z}{t} \right) \left(1 - \exp \left(-\frac{r}{4D_L t} \right) \right) \times \exp \left(-\frac{(z - v_d t)^2}{4D_L t} \right), \quad (6)$$

where r and s represent the radius and surface density of a thin disk of injected ions, respectively, with the latter used as a scaling factor, z is the length of the drift cell, and α is the reaction frequency set to zero.

Comparisons of the ATDs of the mass selected acetylene monomer, dimer, and trimer ions with the calculated profiles are shown in Fig. 5. The measured K_o , at 303 K for the $\text{C}_2\text{H}_2^{+\bullet}$, $(\text{C}_2\text{H}_2)_2^{+\bullet}$, and $(\text{C}_2\text{H}_2)_3^{+\bullet}$ ions are found to be 19.02 ± 0.3 , 14.2 ± 0.4 , and $11.54 \pm 0.3 \text{ cm}^2 \text{ V}^{-1} \text{ s}^{-1}$ corresponding to Ω of 30.2 ± 1.4 , 38.9 ± 1.4 , and $47.9 \pm 1.4 \text{ \AA}^2$, respectively. As shown in Fig. 5, comparisons of both experimental (open circles) and calculated (solid line) ATDs show excellent fits for the monomer $\text{C}_2\text{H}_2^{+\bullet}$ and trimer $(\text{C}_2\text{H}_2)_3^{+\bullet}$ ions indicating the presence of one isomer of for each ion. However, for the $(\text{C}_2\text{H}_2)_2^{+\bullet}$ ions, the experimental ATD is considerably broader than that calculated using the transport equation (Eq. (6)) suggesting the existence of more than one $\text{C}_4\text{H}_4^{+\bullet}$ isomer in the cluster beam. The broadened ATD indicates that the collision cross sections of the $\text{C}_4\text{H}_4^{+\bullet}$ isomers present in the beam are not sufficiently different to be able to resolve their ATDs in our drift cell where isomers with less than 5% difference in collision cross section cannot be resolved.³¹

C. Calculated structures and collision-cross sections of the $\text{C}_4\text{H}_4^{+\bullet}$ ions

The four lowest energy structures of the $\text{C}_4\text{H}_4^{+\bullet}$ ion calculated using the aug-cc-pVDZ basis set are shown in

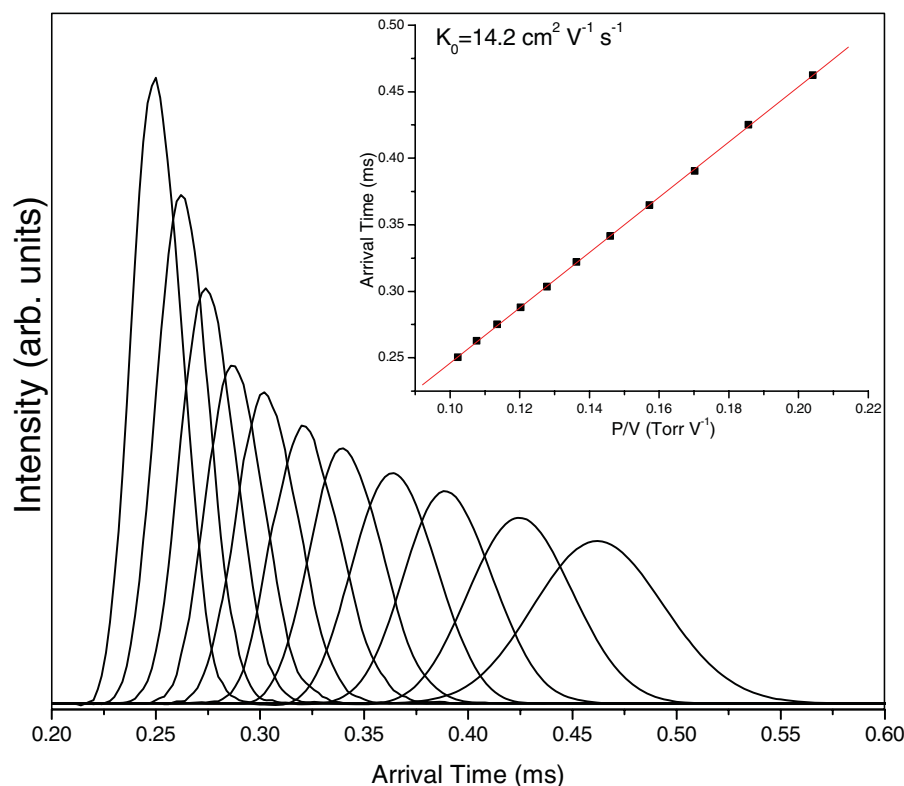


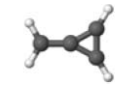
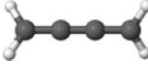
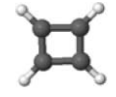
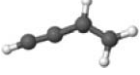
FIG. 4. ATDs of the mass selected acetylene dimer ion at different drift voltages (decreasing from left to right) and helium pressure of 4.1 Torr at 302 K. Inset: plot of t_d versus P/V used in calculating the reduced mobility of the $(\text{C}_2\text{H}_2)_2^{\bullet+}$ ions.

Table I. As expected, the most stable $\text{C}_4\text{H}_4^{\bullet+}$ isomer is the methylenecyclopropene ion (MC, C_{2v}).³⁹ The 1,2,3-butatriene ion (OB, D_2) is the second most stable with a relative energy of 12.2 kJ/mol. The third isomer with a relative energy of 25.8 kJ/mol is the planar cyclobutadiene ion (CB, D_{2h}). Next, is the 1-buten-3-yne ion (vinyl acetylene, VA), predicted to be 37.8 kJ/mol less stable than MC. The fifth most stable $\text{C}_4\text{H}_4^{\bullet+}$ isomer, the methyleneallene ion, is significantly less stable (138.1 kJ/mol relative to MC) than those included in Table I, and therefore is not considered any further.

Interestingly, all the predicted $\text{C}_4\text{H}_4^{\bullet+}$ isomers are of a tight, covalent linear/branched type conformation. No ion–molecule complex of the form $\text{C}_2\text{H}_2^{\bullet+}\text{C}_2\text{H}_2$ was found using the UPBEPBE/aug-cc-pVDZ method. However, it should be noted that the previously predicted $\text{C}_2\text{H}_2^{\bullet+}\text{C}_2\text{H}_2$ complex has a T-type structure (similar to the neutral) with C_{2v} symmetry with intermolecular distance of $\sim 4 \text{ \AA}$.³⁹

The relative energies of the $\text{C}_4\text{H}_4^{\bullet+}$ isomers as predicted by the UPBEPBE/aug-cc-pVDZ method are in qualitative agreement with the results reported from the UQCISD/6-31G* calculations³⁹ but differ from the UB3LYP/6-31G*

TABLE I. Total energy (relative to the energy of the methylenecyclopropene ion), structure, and calculated collision integral (Ω , \AA^2) of the four lowest energy C_4H_4^+ isomers calculated using the DFT/UPBEPBE/aug-cc-pVDZ method. The collision integrals in helium at 300 K are calculated using the trajectory method (Ref. 2).

| | Name | Optimized structures | Relative energy (kJ/mol) | Ω (\AA^2) _{calc} |
|----|-----------------------------|---|--------------------------|---|
| MC | Methylenecyclopropene |  | 0 | 39.9 |
| OB | 1,2,3-Butatriene |  | 12.2 | 41.1 |
| CB | Cyclobutadiene (D_{2h}) |  | 25.8 | 38.6 |
| VA | 1-Buten-3-yne |  | 37.8 | 41.1 |

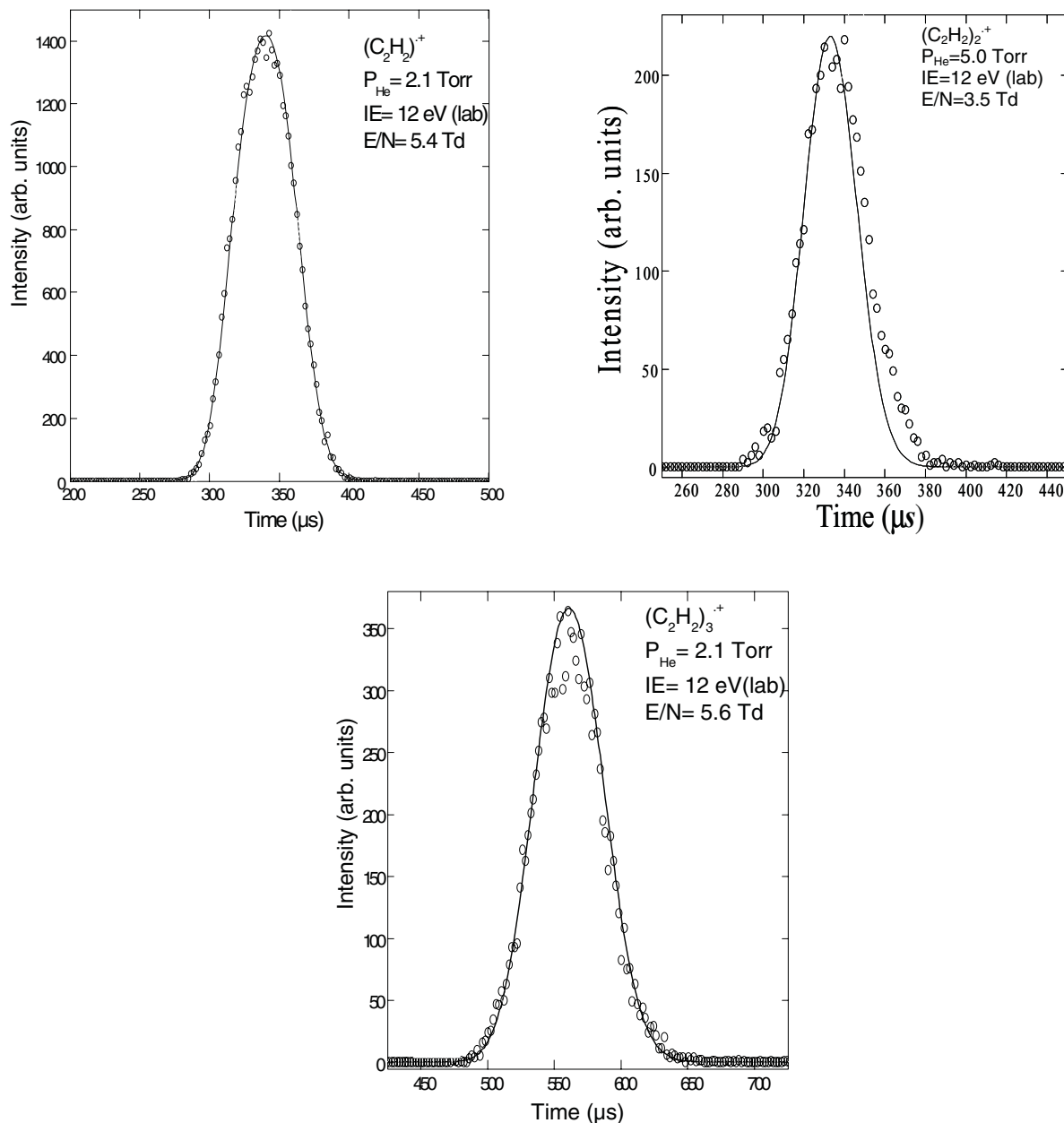


FIG. 5. Comparisons of the experimental ATDs (open circles) of the acetylene monomer, dimer, and trimer ions and the calculated profiles (solid lines) from the transport equation (Eq. (6)) assuming a single structure for each ion.

calculations⁴⁰ where the 1-buten-3-yne ion was predicted to be more stable than the cyclobutadiene ion.

To investigate the identities of the $C_4H_4^{+\bullet}$ isomers present in the cluster beam, the calculated structures were used to obtain average collision cross sections and mobilities using the trajectory calculations.⁴¹ Although the calculated collision cross section of the CB isomer (38.6 \AA^2) is the closest to the measured value ($38.9 \pm 1.4 \text{ \AA}^2$), the experimental error precludes a definitive structural conclusion based only on the calculated cross sections. Also, the experimental ATD of the $C_4H_4^{+\bullet}$ ion indicates the presence of more than one isomer and therefore, a single isomer with a cross section that perfectly matches the experimental value will not reproduce the experimental ATD. To illustrate this point, the calculated mobility for each isomer was used to calculate the corresponding ATD (Eq. (6)) for comparison with the exper-

imental ATD. The effective time the ions spent outside the drift cell (t_o) (obtained from the intercept of the plot of the drift time (t_d) versus P/V , Eq. (4)) was added to the calculated ATD of each isomer for comparison with the experimental ATD. The results are shown in Fig. 6. As expected, the calculated ATD of the CB isomer is the closest to the experimental ATD because of the similar mobility. The other three isomers show displacements from the experimental ATD due to the differences between the calculated and experimental mobilities. However, none of the four isomers alone including CB is able to reproduce the experimental ATD of the $C_4H_4^{+\bullet}$ ion. This is consistent with the broadened ATD shown in Fig. 5 resulting from the presence of more than one isomer of the $C_4H_4^{+\bullet}$ ion in the experiment.

To investigate the possibility of the presence of more than one $C_4H_4^{+\bullet}$ isomer in the ionized acetylene cluster beam,

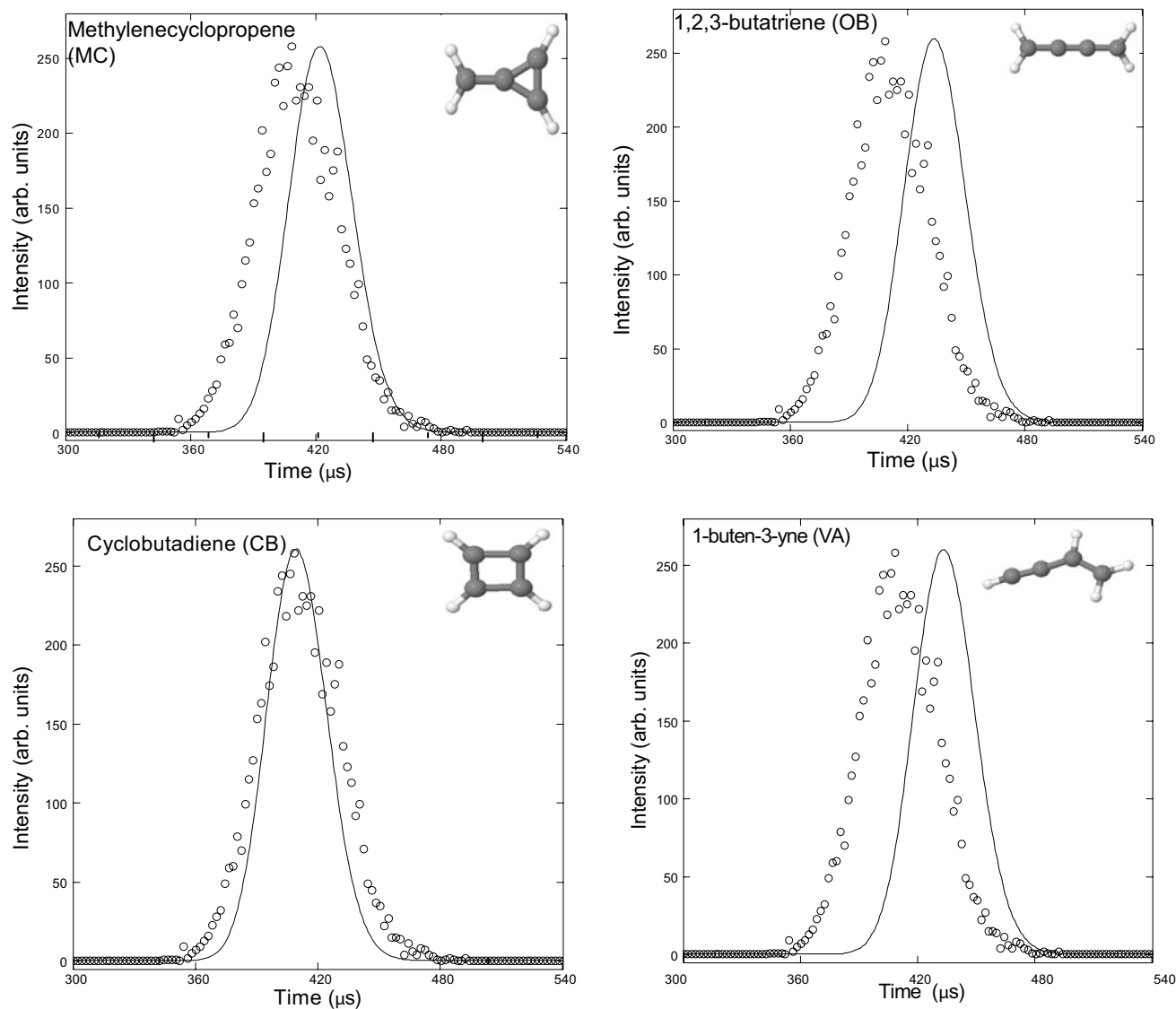


FIG. 6. Comparisons of the experimental ATD of the $(C_2H_2)_2^{*+}$ ions (open circles) and the calculated ATDs (solid lines) for the four lowest energy isomers of the $C_4H_4^{*+}$ ion. The effective time the ions spent outside the drift cell was added to the calculated ATD of each isomer for comparison with the experimental ATD.

hypothetical relative concentrations of all combinations of the four lowest energy isomer pairs were fitted to the experimental ATD. For example, MC and CB at different relative concentrations (50:50, 40:60, 30:70, etc.) were fitted to the experimental ATD. Of all six $C_4H_4^{*+}$ isomer combinations, only mixtures containing the cyclobutadiene ion in combination with the 1-buten-3-yne (vinyl acetylene) ion gave excellent fits to the experimental ATDs as shown in Fig. 7. Slightly reasonable fits could be also obtained by using combinations of the cyclobutadiene and the 1,2,3-butatriene ions as shown in the supplementary material.⁴² It is interesting to note that combinations containing methylenecyclopropene ion, the most stable $C_4H_4^{*+}$ isomer, with other low energy isomers resulted in poor fits as shown in the supplementary material.⁴² Because of the similarity of the calculated collision cross section of CB and the experimental value, isomer combinations containing CB are expected to result in an averaged collision cross section close to the experimental value ($38.9 \pm 1.4 \text{ \AA}^2$). However, as indicated earlier, a successful

pair of isomers should be able to reproduce the width of the experimental ATD and not only the peak maximum which determines the mobility value. Therefore, based on the comparison of the experimental and calculated ATDs, it appears that the $C_4H_4^{*+}$ isomers produced in the ionized acetylene clusters under our experimental conditions are the cyclobutadiene and vinyl acetylene ions.

The mechanism of formation of the cyclobutadiene and vinyl acetylene ions involves intracluster ion-molecule reactions of the $C_2H_2^{*+}$ ion with the neutral acetylene molecule in the cluster. Energy transfer to the low frequency cluster modes leading to evaporation of neutral acetylene molecules can dissipate the excess energy resulting from the covalent addition reactions producing the cyclobutadiene and vinyl acetylene ions. In this way, these isomers can be stabilized within the cluster by evaporative cooling which is analogous to collisional stabilization of the ionic intermediates in the gas phase at high pressures.³⁹ Formation of the cyclobutadiene ion is the most kinetically favored pathway for all the low

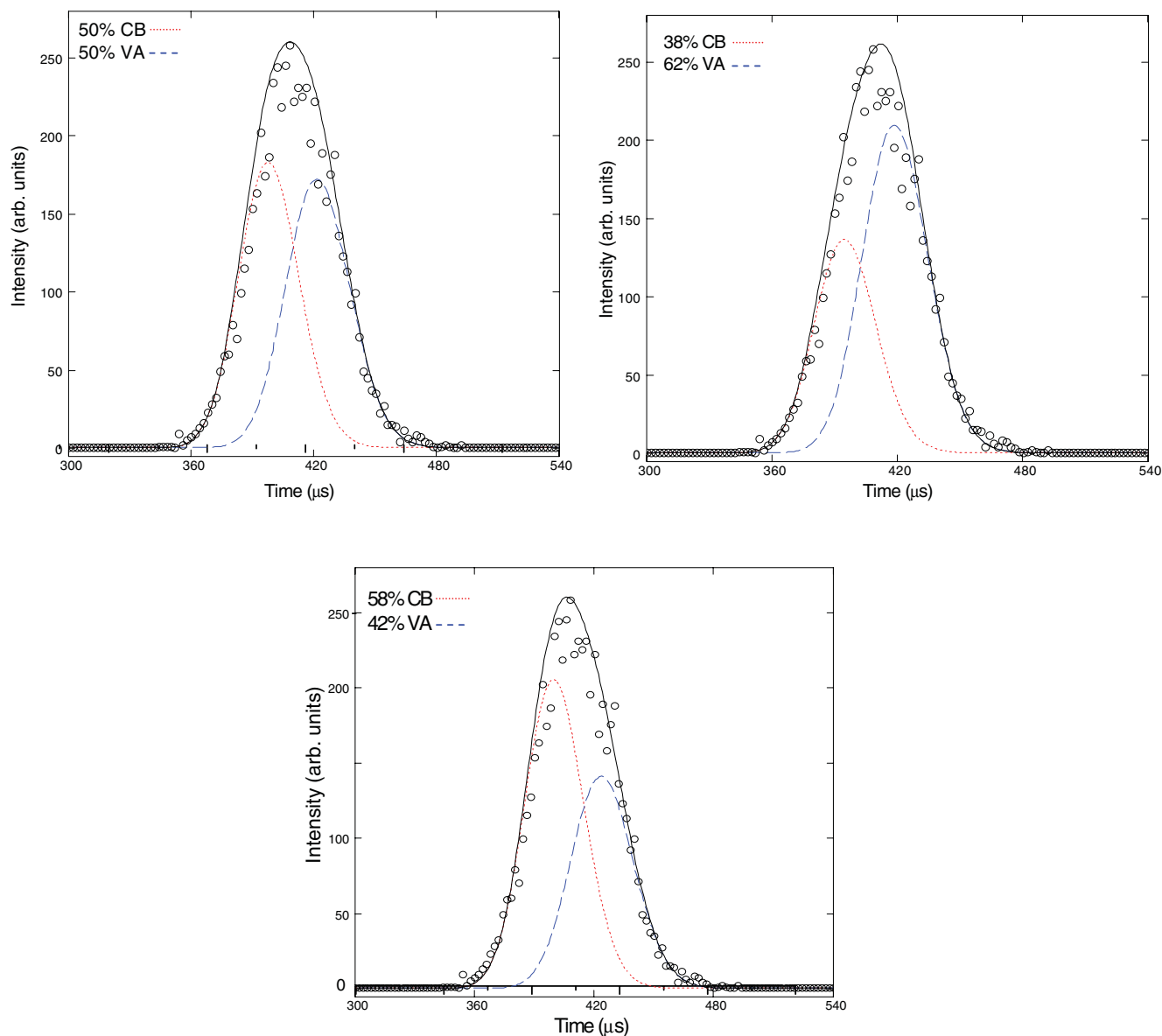


FIG. 7. Comparisons of experimental ATDs of the $(\text{C}_2\text{H}_2)_2^{+\bullet}$ ions (open circles) and the calculated ATDs for different combinations of the cyclobutadiene (CB) and the vinyl acetylene (VA) isomers (solid lines). In order to account for the effective time the ions spend outside the drift cell, the peak maximum of the combined ATDs of each isomer pair was adjusted to coincide with the peak maximum of the experimental ATD.

energy $\text{C}_4\text{H}_4^{+\bullet}$ isomers as it is the only isomer that requires no H shift from its precursor cluster ion, $\text{C}_2\text{H}_2^{+\bullet} + \text{C}_2\text{H}_2$.^{39,43} Therefore, intracuster cyclization to produce the cyclobutadiene ion is expected to be kinetically driven (within the time frame of our experiment) since the heat produced by dimerization of the loose $\text{C}_2\text{H}_2^{+\bullet} + \text{C}_2\text{H}_2$ complex can be efficiently dissipated by evaporation of neutral acetylene molecules from the cluster. In fact, Ono and Ng described a van der Waals type well for the loose $\text{C}_2\text{H}_2^{+\bullet} + \text{C}_2\text{H}_2$ ion;⁴³ which may favor a cyclobutadiene ion route on the reaction coordinate if excess energy dissipation is efficient. Efficient stabilization of the cyclobutadiene ion by evaporation of acetylene molecules from the cluster is analogous to condensed-phase conditions where the cyclobutadiene ion formation is the favorable product.^{44,45}

The second $\text{C}_4\text{H}_4^{+\bullet}$ isomer suggested by the current mobility experiment, the vinyl acetylene ion, is consistent with

the results of Ono and Ng using photoionized acetylene clusters where a linear $\text{C}_4\text{H}_4^{+\bullet}$ isomer was identified as the vinyl acetylene ion.⁴³ Also, photoelectron-photoion coincidence experiments by Booze and Baer²³ concluded that the $\text{C}_4\text{H}_4^{+\bullet}$ species resulting from photoionization of acetylene clusters are likely to be the cyclobutadiene ion in addition to the vinyl acetylene or butatriene ions. Furthermore, detailed theoretical investigation of the C_4H_4^+ potential energy surface by Hrouda *et al.*³⁹ concluded that isomerization of the $(\text{C}_2\text{H}_2)_2^{+\bullet}$ to cyclobutadiene is kinetically more favorable than any of the other $\text{C}_4\text{H}_4^{+\bullet}$ isomers due to the absence of H shifts in its production. Finally, the most recent results Relph *et al.*, using infrared predissociation spectroscopy in conjunction with harmonic frequency calculations, showed that the $\text{C}_4\text{H}_4^{+\bullet}$ ion produced by sequential addition of acetylene molecule onto the $\text{C}_2\text{H}_2^{+\bullet}$ ion is predominantly present as the cyclobutadiene cation.²⁸

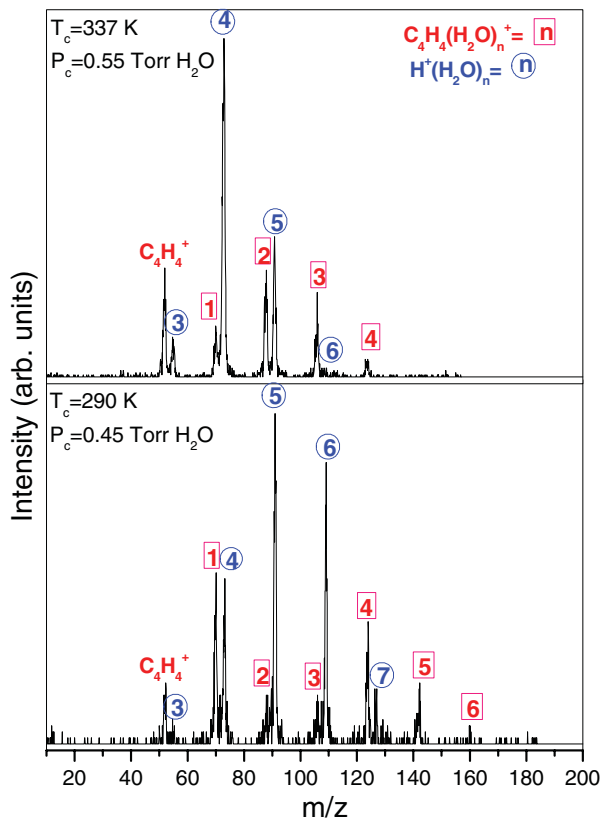


FIG. 8. (Top) Mass spectrum resulting from the injection (15.4 eV) of mass selected dimer clusters into the drift cell containing 0.55 Torr H_2O at 337 K. (Bottom) Mass spectrum resulting from the injection (15.4 eV) of mass selected dimer clusters into the drift cell containing 0.45 Torr H_2O at 290 K.

D. Stepwise hydration of the $\text{C}_4\text{H}_4^{\bullet+}$ ion

To shed more light on the identity of the $(\text{C}_2\text{H}_2)_2^{\bullet+}$ ion formed from the ionization of acetylene clusters, we studied the sequential addition of water molecules onto the $(\text{C}_2\text{H}_2)_2^{\bullet+}$ ion under thermal conditions. Figure 8 displays the mass spectra obtained upon injection of the mass selected $(\text{C}_2\text{H}_2)_2^{\bullet+}$ into the drift cell containing water vapor at 0.55 Torr (337 K) and 0.45 Torr (290 K). At these temperatures (337 and 290 K), the main peaks observed are the dimer and its hydrated ions, $(\text{C}_2\text{H}_2)_2^{\bullet+}(\text{H}_2\text{O})_n$ with $n = 1-4$ at 337 K ($n = 1-6$ at 290 K) and protonated water clusters, $\text{H}^+(\text{H}_2\text{O})_n$ with $n = 3-6$ at 337 K ($n = 3-7$ at 290 K).

The hydrated $(\text{C}_2\text{H}_2)_2^{\bullet+}(\text{H}_2\text{O})_n$ ions are formed according to the stepwise association reaction (7), and the protonated water clusters $\text{H}^+(\text{H}_2\text{O})_n$ are attributed to proton transfer reactions within the $\text{C}_4\text{H}_4^{\bullet+}(\text{H}_2\text{O})_n$ clusters with $n \geq 3$ according to reaction (8). These reactions have been observed for the hydrated benzene cation $\text{C}_6\text{H}_6^{\bullet+}(\text{H}_2\text{O})_n$ and hydrated acetylene trimer ion $(\text{C}_2\text{H}_2)_3^{\bullet+}(\text{H}_2\text{O})_n$ with $n \geq 4$.^{26,30}

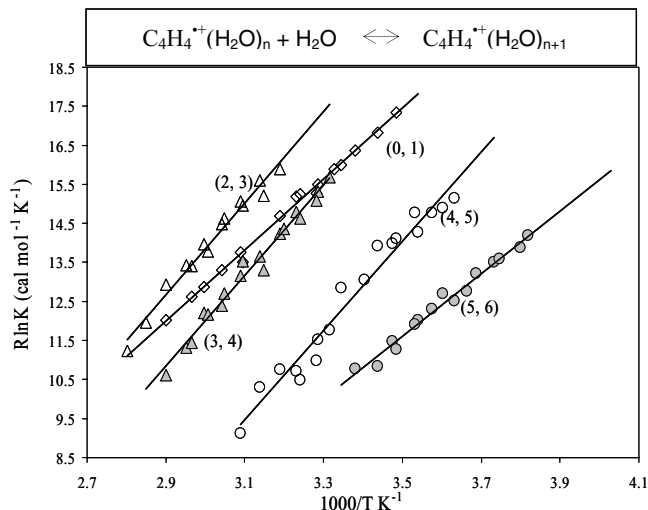
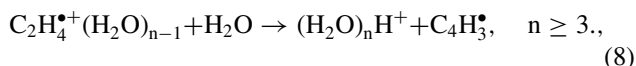
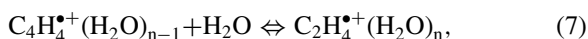


FIG. 9. van't Hoff plots of the temperature dependence of the equilibrium constant of the stepwise hydration of the $\text{C}_4\text{H}_4^{\bullet+}$ ion.

The observation of the deprotonation reaction (8) within the $\text{C}_2\text{H}_4^{\bullet+}(\text{H}_2\text{O})_n$ clusters with $n \geq 3$ indicates that the proton affinity of the radical generated by the deprotonation of the $\text{C}_4\text{H}_4^{\bullet+}$ ion is lower than that of the water trimer (218 kcal/mol).³⁰

Figure 9 displays van't Hoff plots for the stepwise association of reaction (7), and the resulting $\Delta H_{n-1,n}^\circ$ and $\Delta S_{n-1,n}^\circ$ are given in Table II. The $\Delta H_{1,2}^\circ$ and $\Delta S_{1,2}^\circ$ values could not be measured due to diminished ion count of the $\text{C}_4\text{H}_4^{\bullet+}(\text{H}_2\text{O})_2$ cluster as a result of the proton transfer reaction with the next water molecule to generate the $(\text{H}_2\text{O})_3\text{H}^+$ ion. It is clear that the binding energies of the $\text{C}_4\text{H}_4^{\bullet+}(\text{H}_2\text{O})_n$ clusters change little from $n = 1$ to 5, similar to the hydration behavior observed for the benzene ion.⁴¹ This can be explained by the presence of multiple binding sites with comparable energies for the water molecules to attach to the $\text{C}_4\text{H}_4^{\bullet+}$ cation and, by the similarity of the bonding strength between the $\text{C}_4\text{H}_4^{\bullet+}$ ion–water and between water–water interactions. The measured $\Delta S_{3,4}^\circ$, and $\Delta S_{4,5}^\circ$ values of -95.3 , and $-108.2 \text{ J mol}^{-1} \text{ K}^{-1}$ also suggest the formation of adducts with restrained water molecules particularly for $\text{C}_4\text{H}_4^{\bullet+}(\text{H}_2\text{O})_5$ cluster.^{30,46} The significant entropy loss for the addition of the fifth water molecule could be explained by the formation of a cyclic water pentamer within the $\text{C}_4\text{H}_4^{\bullet+}(\text{H}_2\text{O})_5$ cluster. This is consistent the model potential/DFT investigation by Hodges and Stone which found the lowest structures of the $n = 4$ and 5 clusters of $\text{H}_3\text{O}^+(\text{H}_2\text{O})_n$ to be cyclic.⁴⁷ The drop in the binding energy of the sixth water molecule ($\Delta H_{5,6}^\circ$) by approximately 14 kJ/mol and the drop in the $-\Delta S_{5,6}^\circ$ value (Table II) suggest a structure in which the sixth water molecule perhaps hangs loose and interacts weakly with the $\text{C}_4\text{H}_4^{\bullet+}(\text{H}_2\text{O})_5$ cluster. This suggests that the $\text{C}_4\text{H}_4^{\bullet+}(\text{H}_2\text{O})_5$ cluster could consist of a cyclobutadiene cation hydrogen bonded to a cyclic water pentamer. As discussed in Sec. IV C, both the cyclobutadiene and the vinyl acetylene isomers are expected to be major constituents of the $\text{C}_4\text{H}_4^{\bullet+}$ ion in our cluster beam. The measured binding energy for the $\text{C}_4\text{H}_4^{\bullet+} \cdot \text{H}_2\text{O}$ cluster, $38.0 \pm 4 \text{ kJ/mol}$, is in excellent agreement with the G3(MP2)

TABLE II. Measured thermochemistry ($\Delta H_{n-1,n}^\circ$ and $\Delta S_{n-1,n}^\circ$) of hydration reaction (7).

| n | Thermochemical data ^a | |
|-----|----------------------------------|--------------------------|
| | $\Delta H_{n-1,n}^\circ$ | $\Delta S_{n-1,n}^\circ$ |
| 1 | -38.7 | -61.8 |
| 2 | -(38.5-40.3) ^b | |
| 3 | -48.9 | -89.0 |
| 4 | -48.1 | -95.3 |
| 5 | -47.6 | -108.2 |
| 6 | -33.6 | -69.6 |

^aUnits are ΔH° (kJ/mol); ΔS° (J/mol K). Estimated error: $\Delta H^\circ \pm 4$ kJ/mol, $\Delta S^\circ \pm 10$ J/mol K.

^bBased on G3(MP2) calculated binding energies for CB-2W and VA-2W since $\Delta H_{1,2}^\circ$ and $\Delta S_{1,2}^\circ$ values could not be measured due to diminished ion count of the $C_4H_4^{*\+}(H_2O)_2$ cluster resulting from the deprotonation reaction (8).

calculated binding energies for selected $C_4H_4^{*\+} \cdot H_2O$ clusters as presented in the next section.

E. Calculated structures of the hydrated ions $C_4H_4^{*\+}(H_2O)_n$ for $n = 1-2$

The G3//MP2 predicted geometries of the $C_4H_4^{*\+} \cdot H_2O$ complex for the four most stable $C_4H_4^{*\+}$ isomers are shown in Table III.

The most stable hydrated methylenecyclopropene complex (MC-W) consists of a carbon based $CH^{\delta+} \dots OH_2$ hydrogen bond (2.0 Å) to one of the methylenecyclopropene hydrogens. Mulliken charge analysis³⁵ shows that the charge remains on the methylenecyclopropene radical cation. The calculated $CH^{\delta+} \dots OH_2$ binding energy is 11.0 kcal/mol. The hydrated cyclobutadiene ion (CB-W) exhibits a $CH^{\delta+} \dots OH_2$ length of 2.1 Å with a calculated binding energy of 41.0

TABLE III. Optimized structures of the $C_4H_4^{*\+} \cdot H_2O$ species for selected $C_4H_4^{*\+}$ isomers using the G3(MP2) method. Energies are relative to the most stable species for a particular $C_4H_4^{*\+}$ isomer. Binding energies are for the removal of a water molecule from $C_4H_4^{*\+}(H_2O)$ cluster.

| Name | Optimized structures | Binding energies (kJ/mol) ^a |
|------|----------------------|--|
| MC-W | | 46.0 |
| CB-W | | 41.0 |
| OB-W | | 41.4 |
| VA-W | | 49.7 |

^aAll energies are ZPE corrected.

kJ/mol in excellent agreement with the measured binding energy of 38.7 ± 4 kJ/mol. However, no conclusive evidence regarding the $C_4H_4^{*\+}$ isomer identification can be drawn from the calculated binding energies of the hydrated structures since the four hydrated $C_4H_4^{*\+}$ isomers have binding energies within the experimental uncertainty. For example, the hydrated 1,2,3-butatriene ion (OB-W) complex consists of a $CH^{\delta+} \dots OH_2$ (2.1 Å) type hydrogen bond with a binding energy of 41.4 kJ/mol. The final $C_4H_4^{*\+} \cdot H_2O$ complex investigated was that of the 1-buten-3-yne ion (VA-W) where the lowest energy structure has a $CH^{\delta+} \dots OH_2$ (1.9 Å) type hydrogen bond and a significantly higher binding energy (11.9 kcal/mol) compared to the other three $C_4H_4^{*\+}$ isomers. Although the 1-buten-3-yne radical ion is expected to be the other $C_4H_4^{*\+}$ isomer in our beam, the predicted binding energy of 49.7 kJ/mol is significantly larger than the measured value of 38.0 kJ/mol.

The G3//MP2 predicted geometries, relative energies and binding energies for selected $C_4H_4^{*\+}(H_2O)_2$ clusters are displayed in Table IV. The most stable bi-hydrated methylenecyclopropene ion, MC-2Wa, has two $CH^{\delta+} \dots OH_2$ hydrogen bonds with similar bond lengths of 1.9 Å; shorter than that of the mono-hydrated analog MC-W (2.0 Å). Other stable structures, MC-2Wb and MC-2Wc are, respectively, 4.2 and 5.0 kJ/mol less stable than MC-2Wa. It is clear that the second water molecule prefers to form a second hydrogen bond with the MC ion rather than with the first water molecule. The same trend is observed in the bi hydrated cyclobutadiene structures where the most stable isomer CB-2Wa has two bifurcated $CH^{\delta+} \dots OH_2$ bonds opposite to each other with bond lengths (2.2 and 2.1 Å) similar to the bond length of the first water molecule CB-W (2.1 Å). The second stable structure has two H-bonds with the two water molecules through the opposite hydrogen atoms of the CB ion. The third stable structure CB-2Wc involves water-water hydrogen bonding and is less stable than the structures involving H-bonds to the CB ion. The most stable structure for the hydrated 1,2,3-butatriene cluster (OB-2Wa) consists of two carbon based bifurcated $CH^{\delta+} \dots OH_2$ hydrogen bonds with bond lengths of 1.5 and 1.6 Å, significantly shorter than that of the mono-hydrated ion OB-W (2.1 Å). For the final bi-hydrated $C_4H_4^{*\+}$ isomer investigated (1-buten-3-yne, VA), the most stable structure consists of the second water molecule forming a $CH^{\delta+} \dots OH_2$ hydrogen bond across from the mono-hydrated unit. It is interesting to note that in all cases, none of the most stable structures of the bi-hydrated ions are "externally" solvated.³⁰ In other words, the most stable structures consist of arrangements in which both water molecules are directly bound to the $C_4H_4^{*\+}$ ion rather than to another water molecule. This trend is somewhat different from the ROHF/6-31+G** predictions for hydrated benzene cation.³⁰

V. SUMMARY AND CONCLUSIONS

The structure and hydration of the $C_4H_4^{*\+}$ ion formed by electron impact ionization of neutral acetylene clusters have been investigated using the mass-selected ion mobility technique. The mobility measurement indicates the presence of

TABLE IV. G3(MP2) structures of the $C_4H_4^{\bullet+}(H_2O)_2$ clusters for selected $C_4H_4^{\bullet+}$ isomers. Energies are relative to the most stable species for a particular $C_4H_4^{\bullet+}$ isomer. Binding energies are for removal of a water molecule from $C_4H_4^{\bullet+}(H_2O)_2$.

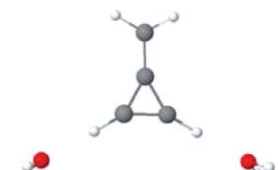
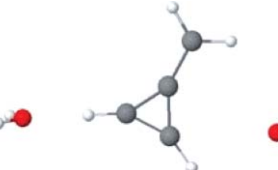
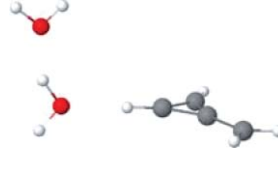

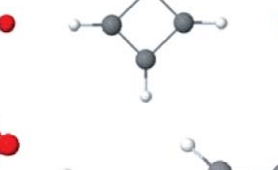
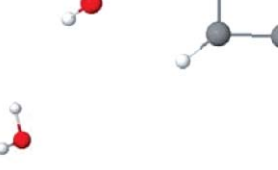
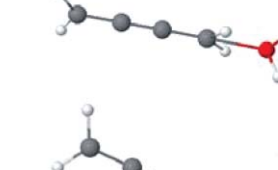
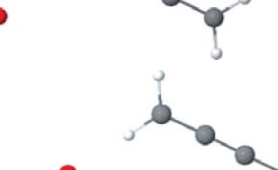
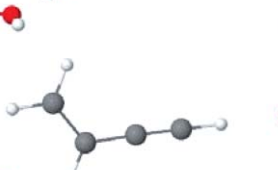


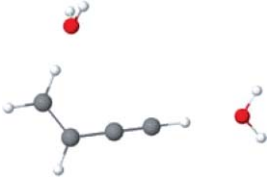
| Name | Optimized structures | Relative energies (kJ/mol) | Binding energies (kJ/mol) ^a |
|--------|---|----------------------------|--|
| MC-2Wa |  | 0.0 | 42.2 |
| MC-2Wb |  | 4.2 | 37.6 |
| MC-2Wc |  | 5.0 | 37.0 |
| CB-2Wa |  | 0.0 | 38.5 |
| CB-2Wb |  | 1.7 | 36.5 |
| CB-2Wc |  | 2.5 | 35.9 |
| OB-2Wa |  | 0 | 38.5 |
| OB-2Wb |  | 0.8 | 38.0 |
| OB-2Wc |  | 2.5 | 35.9 |
| VA-2Wa |  | 0 | 40.3 |

TABLE IV. (Continued)

| Name | Optimized structures | Relative energies (kJ/mol) | Binding energies (kJ/mol) ^a |
|--------|---|----------------------------|--|
| VA-2Wb |  | 2.2 | 48.0 |
| VA-2Wc |  | 5.4 | 34.7 |

^aAll energies are ZPE corrected.

more than one isomer for the $C_4H_4^{\bullet+}$ ion in the cluster beam. The measured average collision cross section of the $C_4H_4^{\bullet+}$ isomers in helium ($38.9 \pm 1.4 \text{ \AA}^2$) is consistent with the calculated cross sections of the four most stable covalent structures calculated for the $C_4H_4^{\bullet+}$ ion [methylene cyclopropene (39.9 \AA^2), 1,2,3-butatriene (41.1 \AA^2), cyclobutadiene (38.6 \AA^2), and vinyl acetylene (41.1 \AA^2)]. However, none of the single isomers is able to reproduce the experimental arrival time distribution of the $C_4H_4^{\bullet+}$ ion. Combinations of cyclobutadiene and vinyl acetylene isomers show excellent agreement with the experimental mobility profile and the measured collision cross section. The fragment ions obtained by the dissociation of the $C_4H_4^{\bullet+}$ ion are consistent with the cyclobutadiene structure. Both the ion mobility and dissociation experiments suggest the presence of the cyclobutadiene structure in agreement with the vibrational predissociation spectrum of the acetylene dimer cation ($(C_2H_2)_2^{\bullet+}$).²⁸

The stepwise hydration experiments show that both the $C_4H_4^{\bullet+}(H_2O)_n$ clusters with $n = 1-6$ and $H^+(H_2O)_n$ clusters with $n = 3-6$ are formed. The protonated water clusters are generated by dissociative proton transfer reactions within the $C_4H_4^{\bullet+}(H_2O)_n$ clusters with $n \geq 3$. The measured binding energy of the $C_4H_4^{\bullet+} \cdot H_2O$ cluster, $38.7 \pm 4 \text{ kJ/mol}$, is in excellent agreement with the G3(MP2) calculated binding energy of cyclobutadiene $^{\bullet+} \cdot H_2O$ cluster (41 kJ/mol). The binding energies of the $C_4H_4^{\bullet+}(H_2O)_n$ clusters change little from $n = 1$ to 5 ($39-48 \text{ kJ/mol}$) suggesting the presence of multiple binding sites with comparable energies for the water- $C_4H_4^{\bullet+}$ and water-water interactions. A significant entropy loss is measured for the addition of the fifth water molecule suggesting a structure with restrained water molecules probably a cyclic water pentamer, within the $C_4H_4^{\bullet+}(H_2O)_5$ cluster. Consequently, a drop in the binding energy of the sixth water molecule is observed suggesting a structure in which the sixth water molecule interacts weakly with the $C_4H_4^{\bullet+}(H_2O)_5$ cluster, presumably consisting of a cyclobutadiene $^{\bullet+}$ cation hydrogen bonded to a cyclic water pentamer. The combination of ion mobility, dissociation and hydration experiments in conjunction with the theoretical calculations provides strong evidence that the $(C_2H_2)_2^{\bullet+}$ ions are predominantly present as the cyclobutadiene cation with some contribution from the vinyl acetylene cation.

ACKNOWLEDGMENTS

We thank the National Science Foundation (CHE-0911146) and NASA (NNX08AI46G) for the support of this work.

- J. S. Lewis, *Physics and Chemistry of the Solar System* (Academic, New York, 1997).
- W. A. Morgan, Jr., E. D. Feigelson, H. Wang, and M. Frenklach, *Science* **252**, 109 (1991).
- C. Chyba and C. Sagan, *Nature* **355**, 125 (1992).
- T. Y. Brooke, A. T. Tokunaga, H. A. Weaver, J. Crovisier, D. Bockelee-Morvan, and D. Crisp, *Nature* **383**, 606 (1996).
- C. P. McKay and W. J. Borucki, *Science* **276**, 390 (1997).
- H. J. Fraser, M. R. S. McCoustra, and D. A. Williams, *Astronomy & Geophysics* **43**, 10 (2002).
- G. Winnewisser and C. Kramer, *Space Sci. Rev.* **90**, 181 (1999).
- S. A. Sanford, J. Aléon, C. M. O'D. Alexander, T. Araki, S. Bajt, G. A. Baratta, J. Borg, J. P. Bradley, D. E. Brownlee, J. R. Brucato, M. J. Burchell, H. Busemann, A. Butterworth, S. J. Clemett, G. Cody, L. Colangeli, G. Cooper, L. D'Hendecourt, Z. Djouadi, J. P. Dworkin, G. Ferrini, H. Fleckenstein, G. J. Flynn, I. A. Franchi, M. Fries, M. K. Gilles, D. P. Glavin, M. Gounelle, F. Grossemy, C. Jacobsen, L. P. Keller, A. L. D. Kilcoyne, J. Leitner, G. Matrajt, A. Meibom, V. Mennella, S. Mostefaoui, L. R. Nittler, M. E. Palumbo, D. A. Papanastassiou, F. Robert, A. Rotundi, C. J. Snead, M. K. Spencer, F. J. Stadermann, A. Steele, T. Stephan, P. Tsou, T. Tyliczszak, A. J. Westphal, S. Wirick, B. Wopenka, H. Yabuta, R. N. Zare, and M. E. Zolensky, *Science* **314**, 1720 (2006).
- J. H. Waite, Jr., D. T. Young, T. E. Cravens, A. J. Coates, F. J. Crary, B. Magee, and J. Westlake, *Science* **316**, 870 (2007).
- G. C. Sloan, M. Matsuura, A. A. Zijlstra, E. Lagadec, M. A. T. Groenewegen, P. R. Wood, C. Szyszka, J. Bernard-Salas, and J. T. van Loon, *Science* **323**, 353 (2009).
- H. F. Calcote and D. G. Keil, *Pure Appl. Chem.* **62**, 815 (1990).
- E. L. Shock and M. D. Schulte, *Nature* **343**, 728 (1990).
- M. Kalberer, D. Paulsen, M. Sax, M. Steinbacher, J. Dommen, A. S. H. Prevot, R. Fisseha, E. Weingartner, V. Frankevich, R. Zenobi, and U. Baltensperger, *Science* **303**, 1659 (2004).
- P. Ehrenfreund and M. A. Sephton, *Faraday Discuss.* **133**, 277 (2006).
- F. Salama, C. Joblin, and L. J. Allamandola, *Planet. Space Sci.* **43**, 1165 (1995).
- V. Anicich and M. J. McEwan, *Planet. Space Sci.* **45**, 897 (1997).
- E. Herbst, *J. Phys. Chem. A* **109**, 4017 (2005).
- J. Cernicharo, A. M. Heras, A. G. G. M. Tielens, J. R. Pardo, F. Herpin, M. Guelin, and L. B. F. M. Waters, *Astrophys. J.* **546**, L123 (2001).
- G. B. I. Scott, D. A. Fairley, C. G. Freeman, M. J. McEwan, N. G. Adams, and L. M. Babcock, *J. Phys. Chem. A* **101**, 4973 (1997).
- P. M. Woods, T. J. Millar, E. Herbst, and A. A. Zijlstra, *Astron. Astrophys.* **402**, 189 (2003).
- Y. Ono and C. Y. Ng, *J. Am. Chem. Soc.* **104**, 4752 (1982).
- H. Shinohara, H. Sato, and N. Washida, *J. Phys. Chem.* **94**, 6718 (1990).
- J. A. Booze and T. Baer, *J. Chem. Phys.* **98**, 186 (1993).

- ²⁴M. T. Coolbaugh, S. G. Whitney, G. Vaidyanathan, and J. F. Garvey, *J. Phys. Chem.* **96**, 9139 (1992).
- ²⁵P. O. Momoh, S. A. Abrash, R. Mabrouki, and M. S. El-Shall, *J. Am. Chem. Soc.* **128**, 12408 (2006).
- ²⁶P. O. Momoh and M. S. El-Shall, *Chem. Phys. Lett.* **436**, 25 (2007).
- ²⁷P. O. Momoh, A. R. Soliman, M. Meot-Ner, A. Ricca, and M. S. El-Shall, *J. Am. Chem. Soc.* **130**, 12848 (2008).
- ²⁸R. A. Relph, J. C. Bopp, J. R. Roscioli, and M. A. Johnson, *J. Chem. Phys.* **131**, 114305 (2009).
- ²⁹W. Kohn and L. J. Sham, *Phys. Rev.* **140**, A1133 (1965).
- ³⁰Y. M. Ibrahim, M. Meot-Ner, E. H. Alshraeh, M. S. El-Shall, and S. Scheiner, *J. Am. Chem. Soc.* **127**, 7053 (2005).
- ³¹M. J. Rusyniak, Y. M. Ibrahim, D. L. Wright, S. N. Khanna, and M. S. El-Shall, *J. Am. Chem. Soc.* **125**, 12001 (2003).
- ³²P. O. Momoh and M. S. El-Shall, *Phys. Chem. Chem. Phys.* **10**, 4827 (2008).
- ³³J. P. Perdew, K. Burke, and M. Ernzerhof, *Phys. Rev. Lett.* **77**, 3865–3868 (1996).
- ³⁴NIST Chemistry Web Book, *NIST Standard Reference Database Number 69* (National Institute of Standards and Technology, Gaithersburg, MD, 2001–2006) (<http://webbook.nist.gov>).
- ³⁵M. J. Frisch, G. W. Trucks, H. B. Schlegel, G. E. Scuseria, M. A. Robb *et al.*, Revision C.02, Gaussian, Inc., Wallingford, CT, 2004.
- ³⁶C. Lifshitz, D. Gibson, K. Levsen, and I. Dotan, *Int. J. Mass Spectrom. Ion Process.* **40**, 157 (1981).
- ³⁷E. A. Mason and E. W. McDaniel, *Transport Properties of Ions in Gases* (Wiley, New York, 1988).
- ³⁸P. R. Kemper and M. T. Bowers, *J. Am. Soc. Mass. Spectrom.* **1**, 197 (1990).
- ³⁹V. Hrouda, M. Roeselova, and T. Bally, *J. Phys. Chem. A* **101**, 3925 (1997).
- ⁴⁰J. A. Pople, M. Head-Gordon, and K. Raghavachari, *J. Chem. Phys.* **87**, 5968 (1987).
- ⁴¹M. F. Mesleh, J. M. Hunter, A. A. Shvartsburg, G. C. Schatz, and M. F. Jarrold, *J. Phys. Chem.* **100**, 16082 (1996).
- ⁴²See supplementary materials at <http://dx.doi.org/10.1063/1.3592661> for figures of experimental ATDs of the $(C_2H_2)_2^{*+}$ ions and the calculated ATDs for different combinations of the four lowest energy isomers of the $C_4H_4^{*+}$ ion methylenecyclopropene (MC, C_{2v}), 1,2,3-butatriene (OB, D_2), cyclobutadiene (CB, D_{2h}), and 1-buten-3-yne (vinyl acetylene, VA). All combinations of isomer pairs (A,B) with different relative concentrations (A:B = 50:50, 30:70, 38:62, 62:38, and 70:30) were fitted to the experimental ATD using transport theory (equation 7), (30 figures).
- ⁴³Y. Ono and C. Y. Ng, *J. Chem. Phys.* **77**, 2947 (1982).
- ⁴⁴M. Shiotani, K. Ohta, Y. Nagata, and J. Sohma, *J. Am. Chem. Soc.* **107**, 2562 (1985).
- ⁴⁵H. Bock, B. Roth, and G. Maier, *Chem. Ber.* **117**, 172–186 (1984).
- ⁴⁶R. Ludwig, *Angew. Chem. Int. Ed.* **40**, 1808 (2001).
- ⁴⁷M. P. Hodges and A. J. Stone, *J. Chem. Phys.* **110**, 6766 (1999).